Chemistry–A European Journal
Research Article
doi.org/10.1002/chem.202201929
Chemistry Europe
European Chemical Societies Publishing
www.chemeurj.org

Water Sorption Controls Extreme Single-Crystal-to-Single-Crystal Molecular Reorganization in Hydrogen Bonded Organic Frameworks

Stephanie A. Boer,[a, b] Luke Conte,[c] Andrew Tarzia,[d, e] Michael T. Huxley,[d] Michael G. Gardiner,[a] Dominique R. T. Appadoo,[b] Courtney Ennis,[f, g] Christian J. Doonan,[d] Christopher Richardson,*[c] and Nicholas G. White*[a]

Abstract: As hydrogen bonded frameworks are held together by relatively weak interactions, they often form several different frameworks under slightly different synthesis conditions and respond dynamically to stimuli such as heat and vacuum. However, these dynamic restructuring processes are often poorly understood. In this work, three isoreticular hydrogen bonded organic frameworks assembled through charge-assisted amidinium···carboxylate hydrogen bonds ($\mathbf{1}^{C/C}$, $\mathbf{1}^{Si/C}$ and $\mathbf{1}^{Si/Si}$) are studied. Three distinct phases for $\mathbf{1}^{C/C}$ and four for $\mathbf{1}^{Si/C}$ and $\mathbf{1}^{Si/Si}$ are fully structurally characterized. The transitions between these phases involve extreme yet recoverable molecular-level framework reorganization. It is demonstrated that these transformations are related to water content and can be controlled by humidity, and that the non-porous anhydrous phase of $\mathbf{1}^{C/C}$ shows reversible water sorption through single crystal to crystal restructuring. This mechanistic insight opens the way for the future use of the inherent dynamism present in hydrogen bonded frameworks.

Introduction

Inspired by the pioneering work by Ermer[1] and Wuest,[2–3] the field of hydrogen bonded organic frameworks (HOFs), i.e. three-dimensional networks assembled by hydrogen bonds, has seen rapid progress in the past decade.[4–5] HOFs have been touted as promising materials for a range of applications including gas sorption,[6–9] proton conduction,[10–12] sensing[13] and enzyme encapsulation.[14–15] While many of the properties and applications of HOFs are similar to those of metal-organic frameworks (MOFs), the relative weakness of hydrogen bonds compared to metal-ligand coordination bonds means that HOFs are typically prepared in milder conditions, are often more crystalline, and can often be re-dissolved.[4] Although hydrogen bonds may be weak, their flexibility and tolerance to restructuring may give HOFs decided advantages but this is yet to be demonstrated.

Typically only one porous/open form of a HOF has been reported, although examples where different crystallization solvents lead to different framework forms are known, typically arising from different hydrogen bonding arrangements.[16–24] Alternatively, additional structural forms of HOFs can occur when an existing framework undergoes a dynamic process or rearrangement in response to a stimulus such as heat or vacuum.[4] These stimuli often result in structural change, often in conjunction with a change in solvent content in the materials' pores. These changes are most often observed when HOFs are activated in order to study their porosity, and it is notable that while impressive surface areas have been reported

[a] *Dr. S. A. Boer, Dr. M. G. Gardiner, Assoc. Prof. N. G. White*
Research School of Chemistry
Australian National University
Canberra, 2600 ACT (Australia)
E-mail: nicholas.white@anu.edu.au
Homepage: www.nwhitegroup.com

[b] *Dr. S. A. Boer, Dr. D. R. T. Appadoo*
ANSTO Australian Synchrotron
Clayton, 3168 VIC (Australia)

[c] *L. Conte, Assoc. Prof. C. Richardson*
School of Chemistry and Molecular Bioscience
Faculty of Science Medicine and Health
University of Wollongong
Wollongong, 2520 NSW (Australia)
E-mail: chris_richardson@uow.edu.au

[d] *Dr. A. Tarzia, Dr. M. T. Huxley, Prof. C. J. Doonan*
Department of Chemistry and Centre for Advanced Materials
University of Adelaide
Adelaide, 5005 SA (Australia)

[e] *Dr. A. Tarzia*
Department of Chemistry
Molecular Sciences Research Hub
Imperial College London
White City Campus, London, W12 0BZ (UK)

[f] *Dr. C. Ennis*
Department of Chemistry
University of Otago
Dunedin, 9054, New Zealand

[g] *Dr. C. Ennis*
The MacDiarmid Institute for Advanced Materials and Nanotechnology
6140 Wellington (New Zealand)

Supporting information for this article is available on the WWW under https://doi.org/10.1002/chem.202201929

for some HOFs, in many cases seemingly open frameworks show much smaller than expected porosities.[12] When porosity is observed, it is common to observe (by PXRD) a rearrangement of the HOF lattice to a new crystalline phase upon activation,[25] although the molecular structure of this phase is often not determined.

Generally speaking, while dynamic processes in HOFs appear to be common, they have received relatively little attention and yet they are key to understanding and therefore unlocking materials performance. In the more established field of MOF chemistry, dynamic processes have been studied more thoroughly and have been found to be important for many selective and/or gated sorption processes.[26] In few cases have detailed studies of structural changes in HOFs been reported. Cooper and Day showed that four forms of a hydrogen bonded benzimidazolone framework could be accessed, and studied the interconversion of these through temperature changes, and guest removal/addition.[25] Others have observed phase changes on heating/solvent loss/gas sorption and managed to structurally characterize the resulting products,[21,27–31] although it is common to see a loss in crystallinity meaning that single crystal X-ray diffraction could not be used to determine the precise structures for the activated frameworks.

It is noteworthy that many porous HOFs reported are assembled by quite weak hydrogen bonds between neutral molecular components; these materials are stable to heat and often to evacuation but typically dissolve in polar organic solvents.[4] In contrast, HOFs assembled from stronger charge-assisted hydrogen bonds are typically insoluble in organic solvents but are often non-porous or have very low porosities (despite sometimes possessing significant calculated porosities) often due to structural changes upon activation. Notable exceptions include an alkylammonium···sulfonate network[32] and a guanidinium···sulfonate framework,[33] that withstand desolvation without structural reorganization and show microporosity.

We have recently reported the synthesis of frameworks assembled by charge-assisted hydrogen bonding between amidinium cations and carboxylate anions.[34–35] These frameworks can be prepared in a predictable manner, and show good stability to heating to 100 °C in DMSO, boiling water, and aqueous solutions of varying pH.[14,36] However, despite this high stability and moderate-to-high calculated surface areas, we have as yet been unable to obtain permanently porous materials. We saw framework polymorphism for an amidinium···carboxylate framework constructed from terephthalate anion tectons as crystallization from cold water gave an open framework while crystallization from ethanol/water or in warm water gave a denser phase. Furthermore, we observed dynamic processes where the open phase restructures to the denser phase by heating in a solvent.[34] Clearly therefore, dynamic processes exist in frameworks assembled using charge-assisted hydrogen bonds.

In this work, we explore the ability of three isoreticular amidinium···carboxylate HOFs to undergo extreme restructuring in response to temperature and humidity stimuli. We show that three or four distinct crystalline phases are accessible for each of the three frameworks and map the molecular restructuring by diffraction and thermal methods in these stimuli-responsive processes. We also demonstrate reversible high enthalpy water vapour uptake by three-dimensional HOFs.

Results and Discussion

Three hydrogen bonded frameworks were assembled from the organic components shown in Figure 1. These frameworks are referred to as $\mathbf{1}^{C/C}$, $\mathbf{1}^{Si/C}$, and $\mathbf{1}^{Si/Si}$ where the first superscript letter describes whether the central atom of the amidinium tecton is carbon or silicon, while the second superscript letter refers to the carboxylate tecton. We have previously reported the X-ray crystal structures of the "as-synthesized" forms of these frameworks.[36–38] All three frameworks have tetragonal unit cells and consist of six-fold interpenetrated hydrogen bonded nets assembled by $R_2^2(8)$ N-H···O hydrogen bonds. All three frameworks contain square channels, which hold 12 well-ordered water molecules per formula unit in their crystal structures (i.e. tetraamidinium·tetracarboxylate·$12H_2O$).

Thermal dehydration of $\mathbf{1}^{C/C}$

We found that gentle heating under vacuum of as-synthesized $\mathbf{1}^{C/C}$ (which we term α-$\mathbf{1}^{C/C}$) led to a new crystalline phase. To investigate this process further we analyzed α-$\mathbf{1}^{C/C}$ by simultaneous thermogravimetric analysis-differential scanning calorimetry (TGA-DSC). This revealed endothermic mass losses at ~50 and ~100 °C, which together account for the loss of all 12 waters from the structure (Figure 2, calc. 18.0%; found 18.5%). The anhydrous phase is stable to ~250 °C whereupon endothermic expulsion of ammonia from the amidinium component is observed,[39] and the material undergoes thermal decomposition from ~350 °C. The stepwise water losses at relatively low temperature combined with the new phase identified con-

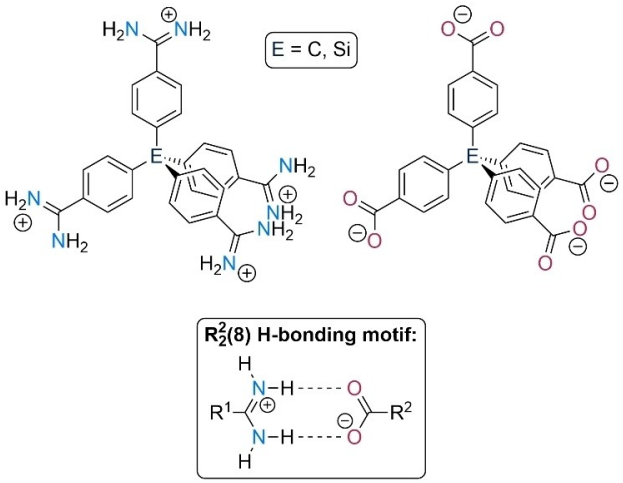

Figure 1. Structures of the molecular building blocks employed and the $R_2^2(8)$ hydrogen bonding motif present in the frameworks.

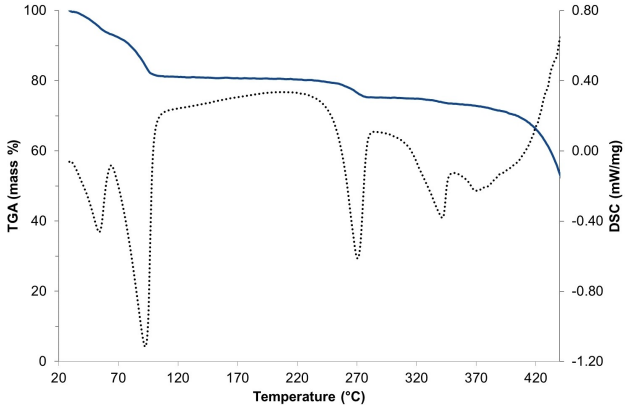

Figure 2. Partial TGA-DSC plot of α-$1^{C/C}$ showing mass losses (blue line) and associated energy changes (dotted black line). The full plot to 600 °C is provided as Figure S21.

firmed structural reorganization during dehydration and we sought to characterize the dehydration processes at the molecular level.

Variable temperature SCXRD studies of $1^{C/C}$

Given the observed mass loss steps in TGA-DSC at accessible temperatures, we studied the framework structure of α-$1^{C/C}$ using variable temperature SCXRD. Crystal structures collected at −173 °C, −123 °C, 0 °C and 40 °C are very similar (Figure 3a) and the water molecules in the channels remain well-ordered even at 40 °C. This is consistent with synchrotron far-IR measurements that show the bulk frameworks contain well-ordered water molecules (see later). When needle-like crystals of α-$1^{C/C}$ are heated to approximately 45 °C while glued to a goniometer pin, they undergo massive plastic deformation (Supporting Information Figure S7).[40] While we could index these crystals to a new tetragonal cell using synchrotron radiation, we were unable to obtain data of sufficient quality to solve the structure. Heating single crystals on a glass slide caused a few to "jump" off the slide,[41] but most simply bent slightly. These slightly bent crystals retained sufficient crystallinity to allow structure determination using synchrotron radiation, which revealed a new phase, which we term β-$1^{C/C}$. The unit cell parameters of this phase matched those of the crystals that deformed on the goniometer pin.

The crystals have changed from an I-centered to primitive tetragonal cell and relatively subtle changes in bond angles have resulted in significant effects on the framework structure. The new phase β-$1^{C/C}$ remains six-fold interpenetrated and connected by $R_2^2(8)$ N–H···O hydrogen bonds (Figure 3b). These hydrogen bonds become slightly shorter (mean N···O distance: 2.77 Å for α-$1^{C/C}$, 2.73 Å for β-$1^{C/C}$) and less linear (mean N-H···O angle: 176° for α-$1^{C/C}$, 156° for β-$1^{C/C}$), which has the overall effect of forcing tectons closer together. Angles at the central carbon atoms of the tectons are further from ideal tetrahedra

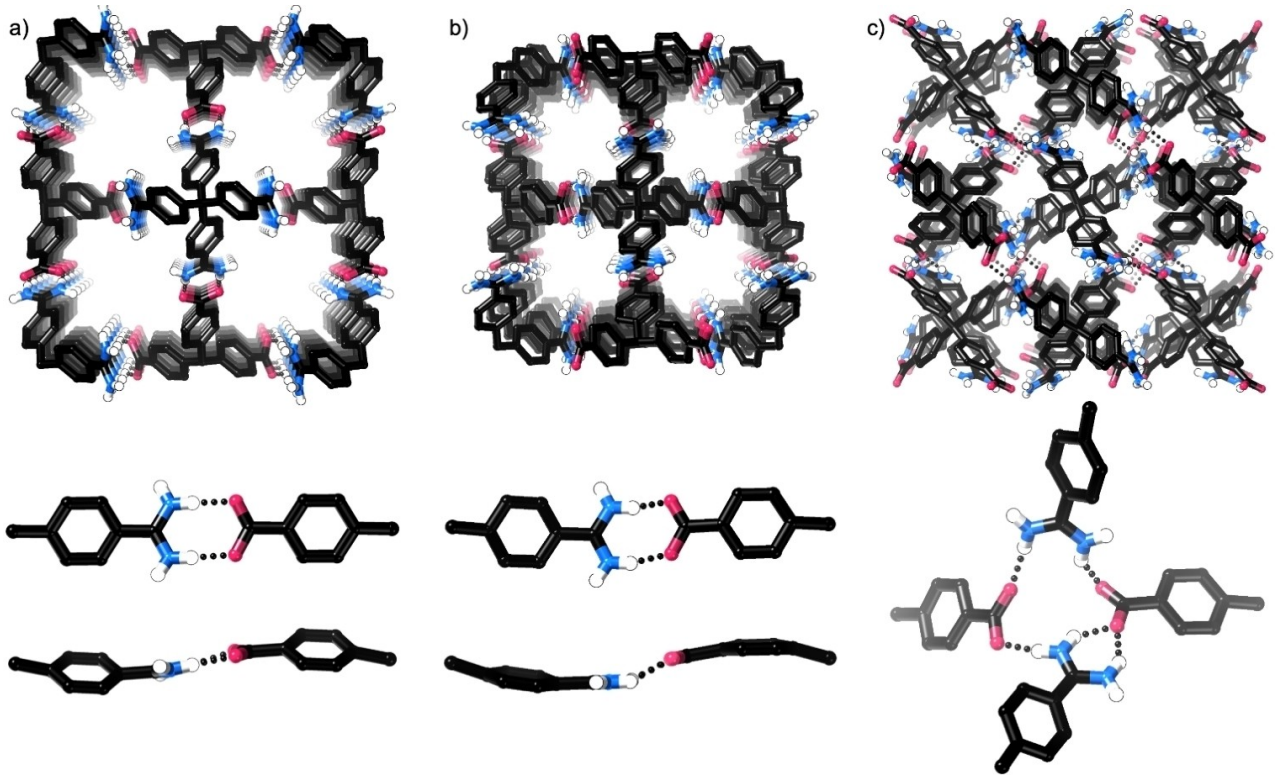

Figure 3. Crystal structures of a) α-$1^{C/C}$ at 100 K, b) β-$1^{C/C}$, c) γ-$1^{C/C}$ showing framework packing (top) and hydrogen bonding arrangements (bottom). Water molecules and most hydrogen atoms omitted for clarity.

(mean deviation from 109.5°: 4.4° for ***β*-1**$^{C/C}$, 3.3° for ***α*-1**$^{C/C}$), which brings the tectons closer together in the *a* and *b* directions but pushes them slightly further apart in the *c* direction. Taken together, these H-bonding and angle changes decrease the size of the square channels parallel to the *c* axis.

This results in a decrease in the calculated water-accessible surface area from 1,330 to 740 $m^2 g^{-1}$. Consistent with the channel constriction, and mass loss observed in TGA-DSC, the SCXRD structure of the β phase contains two full-occupancy and four half-occupancy water molecules per framework unit, rather than the 12 water molecules in the α phase. Notably, even after cooling back to room temperature (or below), the crystals did not revert to the α phase.

Heating single crystals of the β phase causes another thermal transition, this time without deformation, i.e. a single crystal to single crystal transition. While data are of low quality, the structure was determined unambiguously by SCXRD. Remarkably, the framework has undergone extreme molecular restructuring to a close-packed anhydrous phase, which we term ***γ*-1**$^{C/C}$ (Figure 3c), in a single crystal to single crystal process. To achieve this phase the tectons have rotated so that the amidinium and carboxylate groups, which pointed at one another in the α and β phases, are now orthogonal to one another. The $R_2^2(8)$ motif is disrupted and supplanted by a new cyclic hydrogen bonding motif. These changes result in a dense phase with no channels.

Studies of bulk 1$^{C/C}$

Variable temperature PXRD data for bulk microcrystalline **1**$^{C/C}$ were recorded in 10 °C increments from 30 °C to 130 °C and back to 30 °C (Figure 4 shows selected data; see Figure S30 for full data). The dominant phase at or below 40 °C is ***α*-1**$^{C/C}$ while by 50 °C the structure has reorganized to the β phase. This phase is stable until 90 °C, at which point dramatic reorganization to the anhydrous γ phase occurs and remains up to 130 °C (the maximum temperature studied). These phase changes are consistent with the TGA-DSC data, which showed two mass losses at ~50 and 100 °C and no further change up to 250 °C. The γ phase converts to the β phase after cooling (transition complete within 90 minutes at approximately 50% RH; see Figure 4) and this phase appears to be stable indefinitely, i.e. it does not take up more water and revert to the α phase once formed. Clearly the ***γ*-1**$^{C/C}$ to ***β*-1**$^{C/C}$ restructuring is driven by atmospheric moisture adsorption, presumably mediated by favorable interactions with the NH and O donors and ordering within the large channels. To study this further, we carried out TGA-DSC water vapour adsorption measurements.

Further information about the α and β phases was obtained using synchrotron far-IR and mid-IR spectroscopy coupled with DFT calculations. The two phases have distinctly different spectra in the far-IR, attributed to the hydrogen bonding network of water molecules in the channels of the frameworks. The sharp and well-defined nature of these peaks confirms the presence of highly ordered water networks in the channels of both phases (see Supporting Information for further details).

Water vapour sorption of 1$^{C/C}$

Water vapour adsorption measurements on ***γ*-1**$^{C/C}$ were recorded under flowing conditions using TGA-DSC. The isotherm shows one water molecule is taken up at 10% RH before water penetrates at 20% RH (Figure 5) reforming the channels by taking up a further seven water molecules in a process of restructuring to the β phase. Increasing the RH results in further uptake by surface coverage of the crystals but does not result in conversion to the α phase. The desorption leg of the isotherm shows dehydration induced by changing the humidity is not reversible down to 5% RH. The adsorption enthalpy of the major uptake step is 592 $kJ\,mol^{-1}$ (601 $J\,g^{-1}$; see Figure S26), demonstrating that water adsorption results in considerable stabilization of the β phase.

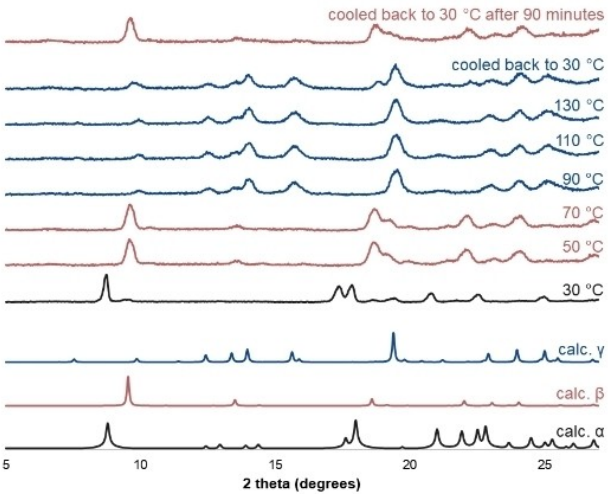

Figure 4. Variable temperature PXRD traces of **1**$^{C/C}$. Traces are colored based on the predominant crystalline phase (α = black, β = red, γ = blue). A version of this plot showing data every 10 °C in heating and cooling cycles is presented in Figure S30.

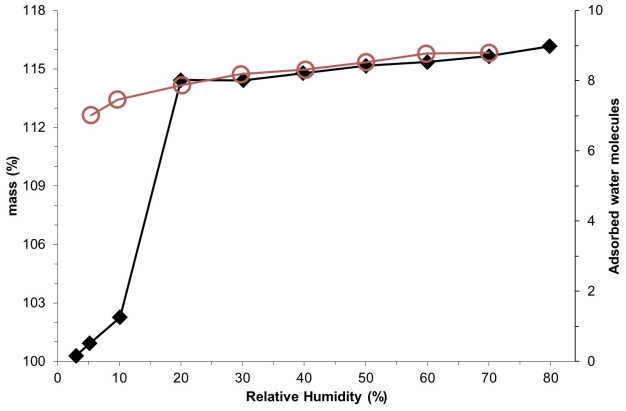

Figure 5. Water vapour isotherm starting from ***γ*-1**$^{C/C}$. Solid symbols represent adsorption. Open symbols represent desorption. Lines are provided to guide the eye.

An experiment starting from α-$\mathbf{1}^{C/C}$ shows water loss starts below 40% RH and equates to approximately six water molecules at 10% RH (Figure S28). This is consistent with restructuring to the β phase. This process is irreversible as raising the humidity results only in surface adsorption. This experiment shows α phase to β phase restructuring is irreversible by humidity control, matching the results from PXRD studies.

Silicon based frameworks $\mathbf{1}^{Si/C}$ and $\mathbf{1}^{Si/Si}$

The silicon-based frameworks $\mathbf{1}^{Si/C}$ and $\mathbf{1}^{Si/Si}$ also adopt α, β, and γ phases in response to thermal dehydration. TGA in combination with PXRD shows the α to β transitions occur at very similar temperatures for $\mathbf{1}^{C/C}$, $\mathbf{1}^{Si/C}$, and $\mathbf{1}^{Si/Si}$, while the β to γ transitions representing complete dehydration occur at slightly lower temperatures for the silicon containing frameworks (80 °C for $\mathbf{1}^{Si/C}$ and 70 °C for $\mathbf{1}^{Si/Si}$), see Figure S22. Interestingly, the reverse transition (i.e. γ to β) takes noticeably longer for frameworks containing silicon based tectons: PXRD studies show that $\mathbf{1}^{C/C}$ has fully returned to the β phase after 90 minutes at 30 °C and approximately 50% RH, while after this time $\mathbf{1}^{Si/C}$ contains a mixture of β and γ, and after this time period only PXRD peaks corresponding to the γ phase of $\mathbf{1}^{Si/Si}$ are visible (Figures S31 and S32). Indeed it takes approximately one day for $\mathbf{1}^{Si/C}$ to return to the β phase and several weeks for $\mathbf{1}^{Si/Si}$ to complete this transition. We suggest this is linked to the more rigid preference for a strict tetrahedral geometry of the silicon centers, which slows down the large geometrical reorganizations necessary for rehydration.[37,42]

Interestingly, a fourth phase was identified for $\mathbf{1}^{Si/C}$ and $\mathbf{1}^{Si/Si}$. Crystals directly from the EtOH/H_2O mother liquor give triclinic unit cells and structures containing large channels, in which satisfactory crystallographic solvent modelling was not possible. However, it appears there are approximately sixteen water and three ethanol solvent molecules per formula unit in these super-swollen frameworks (see Figures S15 and S18).[43] Crystals removed from the solvent for only a few minutes switch to the tetragonal forms, i.e. $\boldsymbol{\alpha}$-$\mathbf{1}^{Si/C}$ and $\boldsymbol{\alpha}$-$\mathbf{1}^{Si/Si}$, containing twelve water molecules.

Discussion

The isoreticular frameworks $\mathbf{1}^{C/C}$, $\mathbf{1}^{Si/C}$ and $\mathbf{1}^{Si/Si}$ show similar but subtly different changes to heat-induced water removal. All three frameworks form kinetically "trapped" α phases with large channel structures containing 12 well-ordered water molecules per formula unit ($\mathbf{1}\cdot 12H_2O$). These phases are stable only to 45-50 °C whereupon they irreversibly convert to β phases through dehydration. Despite this apparent precarity however, α phases are very stable at room temperature and retain this form even after ~1.5 years in a vial at room temperature (as confirmed by PXRD and TGA studies).[44]

Water sorption experiments show that $\boldsymbol{\gamma}$-$\mathbf{1}^{C/C}$ takes up eight water molecules to give the β phase and that this uptake can be reversed by addition of heat. The framework does not take up H_2, N_2 or CO_2 gases (see p32 of Supporting Information) in the γ form and these gases do not invoke restructuring to the β phase. Calculations indicate that the channels in $\boldsymbol{\beta}$-$\mathbf{1}^{C/C}$ are accessible to H_2 and H_2O but inaccessible to N_2 and CO_2 due to their greater kinetic radii. Given that the framework shows uptake of H_2O but not H_2 it is clear that the selectivity for water is not simply size-driven, and we attribute this to reduced interaction enthalpies for gases other than water with the amidinium and carboxylate groups.

Interestingly, the α phase can be converted to the β phase by lowering humidity but lowering humidity to 5% RH is not sufficient to convert the β phase to the anhydrous γ-form (which requires heat or vacuum). The temperature required to thermally dehydrate the frameworks to anhydrous materials decreases from 90 to 80 to 70 °C from $\mathbf{1}^{C/C}$ to $\mathbf{1}^{Si/C}$ to $\mathbf{1}^{Si/Si}$. This ability to control the desorption temperature suggests that these or related frameworks may be useful for water harvesting applications.[45–46]

Conclusion

Molecular level changes induced by dehydration in three hydrogen bonded frameworks have been structurally mapped, with four phases definitively identified for $\mathbf{1}^{Si/C}$ and $\mathbf{1}^{Si/Si}$, and three phases for $\mathbf{1}^{C/C}$. Changes from the triclinic forms of $\mathbf{1}^{Si/C}$ and $\mathbf{1}^{Si/Si}$ to the α phases of these materials, and then from the α to β phases of all three frameworks involve relatively small changes in geometries and hydrogen bonding interactions that cause quite large effects on the dimensions of the framework channels. In contrast, the changes from the β to the γ phases involve massive structural reorganizations, which are reversible and occur with retention of crystallinity. The γ phases reversibly take up water vapour to reverse the structural reorganization, again with retention of crystallinity. This work demonstrates the remarkable ability of frameworks assembled by "weak" interactions such as hydrogen bonds to tolerate drastic restructuring.

Experimental Section

Synthesis, characterization and experimental details are provided as Supporting Information. This includes optimized synthesis of some of organic building blocks and frameworks, and detailed SCXRD, PXRD, TGA-DSC and synchrotron far/mid-IR studies.

Deposition Numbers 2169825 (for α-$\mathbf{1}^{C/C}$ at 100 K), 2169826 (for α-$\mathbf{1}^{C/C}$ at 150 K), 2169827 (for α-$\mathbf{1}^{C/C}$ at 273 K), 2169828 (for α-$\mathbf{1}^{C/C}$ at 313 K), 2169829 (for β-$\mathbf{1}^{C/C}$), 2169830 (for γ-$\mathbf{1}^{C/C}$), 2169831 (for triclinic-$\mathbf{1}^{Si/C}$), 2169832 (for triclinic-$\mathbf{1}^{Si/Si}$) contain the supplementary crystallographic data for this paper. These data are provided free of charge by the joint Cambridge Crystallographic Data Centre and Fachinformationszentrum Karlsruhe Access Structures service.

Acknowledgements

We thank the Australian Research Council for supporting this work (DE170100200, FT210100495 to NGW) and Tobias L. Genet (ANU) for conducting preliminary studies. Parts of this work were conducted using beamlines MX1[47] and MX2[48] of the Australian Synchrotron. This work made use of the Australian Cancer Research Foundation detector. Open Access publishing facilitated by Australian National University, as part of the Wiley - Australian National University agreement via the Council of Australian University Librarians.

Conflict of Interest

The authors declare no conflict of interest.

Data Availability Statement

The data that support the findings of this study are available in the supplementary material of this article.

Keywords: hydrogen bonds · frameworks · molecular reorganization · single crystal to single crystal · supramolecular chemistry

[1] O. Ermer, *J. Am. Chem. Soc.* **1988**, *110*, 3747–3754.
[2] M. Simard, D. Su, J. D. Wuest, *J. Am. Chem. Soc.* **1991**, *113*, 4696–4698.
[3] J. D. Wuest, *Chem. Commun.* **2005**, 5830–5837.
[4] R.-B. Lin, Y. He, P. Li, H. Wang, W. Zhou, B. Chen, *Chem. Soc. Rev.* **2019**, *48*, 1362–1389.
[5] I. Hisaki, C. Xin, K. Takahashi, T. Nakamura, *Angew. Chem. Int. Ed.* **2019**, *58*, 11160–11170; *Angew. Chem.* **2019**, *131*, 11278–11288.
[6] W. Yang, A. Greenaway, X. Lin, R. Matsuda, A. J. Blake, C. Wilson, W. Lewis, P. Hubberstey, S. Kitagawa, N. R. Champness, M. Schröder, *J. Am. Chem. Soc.* **2010**, *132*, 14457–14469.
[7] Y. He, S. Xiang, B. Chen, *J. Am. Chem. Soc.* **2011**, *133*, 14570–14573.
[8] M. Mastalerz, I. M. Oppel, *Angew. Chem. Int. Ed.* **2012**, *51*, 5252–5255; *Angew. Chem.* **2012**, *124*, 5345–5348.
[9] T.-H. Chen, I. Popov, W. Kaveevivitchai, Y.-C. Chuang, Y.-S. Chen, O. Daugulis, A. J. Jacobson, O. Š. Miljanić, *Nat. Commun.* **2014**, *5*, 5131.
[10] W. Yang, F. Yang, T.-L. Hu, S. C. King, H. Wang, H. Wu, W. Zhou, J.-R. Li, H. D. Arman, B. Chen, *Cryst. Growth Des.* **2016**, *16*, 5831–5835.
[11] A. Karmakar, R. Illathvalappil, B. Anothumakkool, A. Sen, P. Samanta, A. V. Desai, S. Kurungot, S. K. Ghosh, *Angew. Chem. Int. Ed.* **2016**, *55*, 10667–10671; *Angew. Chem.* **2016**, *128*, 10825–10829.
[12] G. Xing, T. Yan, S. Das, T. Ben, S. Qiu, *Angew. Chem. Int. Ed.* **2018**, *57*, 5345–5349; *Angew. Chem.* **2018**, *130*, 5443–5447.
[13] I. Hisaki, Y. Suzuki, E. Gomez, Q. Ji, N. Tohnai, T. Nakamura, A. Douhal, *J. Am. Chem. Soc.* **2019**, *141*, 2111–2121.
[14] W. Liang, F. Carraro, M. B. Solomon, S. G. Bell, H. Amenitsch, C. J. Sumby, N. G. White, P. Falcaro, C. J. Doonan, *J. Am. Chem. Soc.* **2019**, *141*, 14298–14305.
[15] G. Chen, S. Huang, Y. Shen, X. Kou, X. Ma, S. Huang, Q. Tong, K. Ma, W. Chen, P. Wang, J. Shen, F. Zhu, G. Ouyang, *Chem* **2021**, *7*, 2722–2742.
[16] K. Kobayashi, A. Sato, S. Sakamoto, K. Yamaguchi, *J. Am. Chem. Soc.* **2003**, *125*, 3035–3045.
[17] C. A. Zentner, H. W. H. Lai, J. T. Greenfield, R. A. Wiscons, M. Zeller, C. F. Campana, O. Talu, S. A. FitzGerald, J. L. C. Rowsell, *Chem. Commun.* **2015**, *51*, 11642–11645.
[18] I. Hisaki, S. Nakagawa, N. Ikenaka, Y. Imamura, M. Katouda, M. Tashiro, H. Tsuchida, T. Ogoshi, H. Sato, N. Tohnai, M. Miyata, *J. Am. Chem. Soc.* **2016**, *138*, 6617–6628.
[19] H. Wang, Z. Bao, H. Wu, R.-B. Lin, W. Zhou, T.-L. Hu, B. Li, J. C.-G. Zhao, B. Chen, *Chem. Commun.* **2017**, *53*, 11150–11153.
[20] P. Li, P. Li, M. R. Ryder, Z. Liu, C. L. Stern, O. K. Farha, J. F. Stoddart, *Angew. Chem. Int. Ed.* **2019**, *58*, 1664–1669; *Angew. Chem.* **2019**, *131*, 1678–1683.
[21] P. Cui, D. P. McMahon, P. R. Spackman, B. M. Alston, M. A. Little, G. M. Day, A. I. Cooper, *Chem. Sci.* **2019**, *10*, 9988–9997.
[22] Q. Yang, Y. Wang, Y. Shang, J. Du, J. Yin, D. Liu, Z. Kang, R. Wang, D. Sun, J. Jiang, *Cryst. Growth Des.* **2020**, *20*, 3456–3465.
[23] Y.-L. Li, E. V. Alexandrov, Q. Yin, L. Li, Z.-B. Fang, W. Yuan, D. M. Proserpio, T.-F. Liu, *J. Am. Chem. Soc.* **2020**, *142*, 7218–7224.
[24] S. Tothadi, K. Koner, K. Dey, M. Addicoat, R. Banerjee, *ACS Appl. Mater. Interfaces* **2020**, *12*, 15588–15594.
[25] A. Pulido, L. Chen, T. Kaczorowski, D. Holden, M. A. Little, S. Y. Chong, B. J. Slater, D. P. McMahon, B. Bonillo, C. J. Stackhouse, A. Stephenson, C. M. Kane, R. Clowes, T. Hasell, A. I. Cooper, G. M. Day, *Nature* **2017**, *543*, 657–664.
[26] S. Kitagawa, K. Uemura, *Chem. Soc. Rev.* **2005**, *34*, 109–119.
[27] H. Wang, B. Li, H. Wu, T.-L. Hu, Z. Yao, W. Zhou, S. Xiang, B. Chen, *J. Am. Chem. Soc.* **2015**, *137*, 9963–9970.
[28] H. Yamagishi, H. Sato, A. Hori, Y. Sato, R. Matsuda, K. Kato, T. Aida, *Science* **2018**, *361*, 1242.
[29] I. Bassanetti, S. Bracco, A. Comotti, M. Negroni, C. Bezuidenhout, S. Canossa, P. P. Mazzeo, L. Marchió, P. Sozzani, *J. Mater. Chem. A* **2018**, *6*, 14231–14239.
[30] P. Cui, E. Svensson Grape, P. R. Spackman, Y. Wu, R. Clowes, G. M. Day, A. K. Inge, M. A. Little, A. I. Cooper, *J. Am. Chem. Soc.* **2020**, *142*, 12743–12750.
[31] Y. Wang, M. Zhang, Q. Yang, J. Yin, D. Liu, Y. Shang, Z. Kang, R. Wang, D. Sun, J. Jiang, *Chem. Commun.* **2020**, *56*, 15529–15532.
[32] A. Comotti, S. Bracco, A. Yamamoto, M. Beretta, T. Hirukawa, N. Tohnai, M. Miyata, P. Sozzani, *J. Am. Chem. Soc.* **2014**, *136*, 618–621.
[33] I. Brekalo, D. E. Deliz, L. J. Barbour, M. D. Ward, T. Friščić, T. Holman, *Angew. Chem. Int. Ed.* **2020**, *59*, 1997–2002; *Angew. Chem.* **2020**, *132*, 2013–2018.
[34] M. Morshedi, M. Thomas, A. Tarzia, C. J. Doonan, N. G. White, *Chem. Sci.* **2017**, *8*, 3019–3025.
[35] N. G. White, *Chem. Commun.* **2021**, *57*, 10998–11008.
[36] S. A. Boer, M. Morshedi, A. Tarzia, C. J. Doonan, N. G. White, *Chem. Eur. J.* **2019**, *25*, 10006–10012.
[37] S. A. Boer, L.-J. Yu, T. L. Genet, K. Low, D. A. Cullen, M. G. Gardiner, M. L. Coote, N. G. White, *Chem. Eur. J.* **2021**, *27*, 1768–1776.
[38] C. Ennis, D. Appadoo, S. A. Boer, N. G. White, *Phys. Chem. Chem. Phys.* **2022**, *24*, 10784–10797.
[39] D. A. Cullen, M. G. Gardiner, N. G. White, *Chem. Commun.* **2019**, *55*, 12020–12023.
[40] For organic crystal-polymer hybrids that reversibly curl on lowering humidity, see: L. Lan, X. Yang, B. Tang, X. Yu, X. Liu, L. Li, P. Naumov, H. Zhang, *Angew. Chem. Int. Ed.* **2022**, *61*, e202200196.
[41] For a report of thoroughly characterized jumping crystals based on a HOF, see: T. Takeda, M. Ozawa, T. Akutagawa, *Angew. Chem. Int. Ed.* **2019**, *58*, 10345–10352; *Angew. Chem.* **2019**, *131*, 10453–10460.
[42] T. Lin, X.-M. Liu, C. He, *J. Phys. Chem. B* **2004**, *108*, 17361–17368.
[43] The unit cell volumes per formula unit are 14 and 13% higher for triclinic-$\mathbf{1}^{Si/C}$ and triclinic-$\mathbf{1}^{Si/Si}$ than for α-$\mathbf{1}^{Si/C}$ and α-$\mathbf{1}^{Si/Si}$, respectively.
[44] See Ref. [33] for a metastable hydrogen bonded framework that remains in its metastable form for 18 years.
[45] H. Kim, S. Yang, S. R. Rao, S. Narayanan, E. A. Kapustin, H. Furukawa, A. S. Umans, O. M. Yaghi, E. N. Wang, *Science* **2017**, *356*, 430–434.
[46] N. Hanikel, X. Pei, S. Chheda, H. Lyu, W. Jeong, J. Sauer, L. Gagliardi, O. M. Yaghi, *Science* **2021**, *374*, 454–459.
[47] N. P. Cowieson, D. Aragao, M. Clift, D. J. Ericsson, C. H. Gee, J. Stephen, N. Mudie, S. Panjikar, J. R. Price, A. Riboldi-Tunnicliffe, R. Williamson, T. Caradoc-Davies, *J. Synchrotron Radiat.* **2015**, *22*, 187–190.
[48] D. Aragao, J. Aishima, H. Cherukuvada, R. Clarken, M. Clift, N. P. Cowieson, D. J. Ericsson, C. L. Gee, S. Macedo, N. Mudie, S. Panjikar, J. R. Price, A. Riboldi-Tunnicliffe, R. Rostan, R. Williamson, T. T. Caradoc-Davies, *J. Synchrotron Radiat.* **2018**, *25*, 885–891.

Manuscript received: June 22, 2022
Accepted manuscript online: June 29, 2022
Version of record online: August 17, 2022